

Application of CFD simulation on various irregular-shaped buildings for determining wind forces and interference effects

Waqr Ismail Shaikh¹, Dr. Sachin B. Mulay²

*Department Of Civil Engineering
Sandip University, Nashik, Maharashtra, India*

*Corresponding Author: er.waqrshaikh@gmail.com

Available online at: <http://www.ijcert.org>

Received: 08/06/2022,

Revised: 21/06/2022,

Accepted: 25/06/2022,

Published: 26/06/2022

Abstract: - Buildings, cooling towers, chimneys, and other tall, thin structures are more vulnerable to wind loads. Wind loads can be increased or decreased by additional structures surrounding these. The interference effect refers to the influence on the primary structure caused by the presence of other structures. The phenomena of interference have acquired importance because of the damage or collapse of structures caused by it. Various experiments and limited computer simulations have studied interference effects on diverse structures. Computational fluid dynamics (CFD) is a better alternative to wind tunnel tests in determining wind loads owing to interference effects on structures. This research considers three structures, two similar structures and one irregular structure such as T-shape with varied wind angles and interfering distances. This study examines various forces and velocity vectors of wind interferences on the structures. Furthermore, using Ansys, a comparative analysis is carried out between Wind Tunnel Test and Computational Fluid Dynamics.

Keywords: Buildings, Wind Interference, Wind Tunnel testing, Computational Fluid Dynamics

1. Introduction

The wind is a significant design factor for civil engineers, architects, and urban planners. Wind risk is significant for high-rise constructions. Coastal cities and other places with significant wind speeds require wind engineering analyses even for smaller urban structures owing to complicated interactions. In most construction projects, these assessments analyze wind loads and pedestrian wind comfort. They can foresee potential harmful impacts and assist enhance designs to mitigate them. Identifying structural and facade loads. This utilizes steady-state modeling to identify high or low peak pressure zones with increased wind forces. For modest building designs, basic coding technique is frequently sufficient for determining pressure loads. Complex geometries and congested urban areas require

numerical analysis (CFD) and wind tunnel testing. Wind load determination and mitigation. Unsteady vortex shedding can cause fluctuating crosswinds on slender high-rises. If these oscillations match the structure's inherent frequency, the motion might be amplified, causing damage or collapse. Standard wind engineering studies involve wind tunnel testing, but an optimum design approach incorporates numerical analysis with CFD as an iterative design supplement. Once an improved building model is developed using CFD modeling, wind tunnel testing begins with many hazards minimized. The CFD tool saves time and money.

CFD models a virtual wind tunnel to quickly analyze pressure and wind loads. Simulation gives 3D contouring and quantitative wind pressure, forces, and speeds. Complex recirculating flow and vortex areas can be enhanced. Advanced boundary layer profiles and mean and peak wind conditions may be predicted. In this new age, buildings are rising higher to conserve space

and become intricate cultural symbols. Architects and engineers developing complex projects must use novel wind modeling techniques. High-fidelity engineering simulation, and CFD in particular, may help evaluate and optimize designs early in the development process to supplement wind tunnel testing to ensure structural safety and sustainability. Using wind tunnel tests and computational fluid dynamics, the study's goal is to compare the impacts of wind interference on many structures (Ansys).

2. Background

A second structure interrupts the wind around the first. The interfering impact alters the wind stresses on the main structure by disrupting the flow. Wind tunnel experiments [1-3] and CFD [4-6] are used to study wind load implications. The model is utilized in ANSYS Fluent as a CFD tool to simulate airflow around the structure in this inquiry. Simulations study interference between two similar buildings, chimneys and wind turbines. These factors are examined using pressure-efficient studies on the major structure at various wind directions and interference distances for the same terrain type. The wind angle, form and orientation of the structure, the distance between structures, terrain type, and other factors determine the risk of interference. This research has sought to characterize the interference phenomena between various structures, which can assist the efficient design of structures to resist wind load fluctuations produced by interference. This chapter includes a literature overview of wind tunnel experiments and CDF testing for irregular and tall buildings.

Thordal, Bennetsen, & Koss (2019) [1] describe how CFD simulations can determine wind loads on high-rise structures. Key atmospheric boundary layer parameters are reviewed to see if a numerical simulation generates enough upstream wind flow. Inflow boundary conditions may be constructed using four major strategies. The newest potential methods are evaluated for flaws and strengths. Comparing numerical and experimental CAARC building outcomes. Shinde & Shingade (2018) [2] researched turbulence modeling and numerical methodologies employing Reynolds-averaged Navier Stokes and Large Eddy Simulation (LES) equations applied to a square prismatic prototype structure was examined in this work.

These numerical algorithms reveal important aerodynamics and improve flow visualization in a virtual environment when coupled with realistic atmospheric boundary layer flow simulation. Hu, Cheng, & Qian (2018) [3] discuss how fast urbanization and expanding construction needs in China have led to growing residential building density and pedestrian discomfort in residential wind environments. To evaluate the link between residential building density and wind

environment, simulated instances of residential structures with varied densities were provided. Computer numerical modeling was used to determine the wind environment of residential areas with varied building densities. Yu, Xie, Zhu, & Gu, (2015) [4] Wind pressure distributions between tandem, oblique, and parallel structures were studied using synchronous pressure measurements. Due to its longer duration, the wind is a more effective lateral load on tall buildings than an earthquake. Sharma & Parekar's (2019) [5] literature suggests analyzing a 200-meter building's wind loads. Due to expensive modeling costs and a lack of appropriate wind tunnels, only a few tall structures are analyzed in wind tunnels. Thordal, Bennetsen, & Koss, (2019) [1] Five different attack angles are studied in experimental and digital wind tunnels to determine how much wind the CAARC structure can withstand.

The Large Eddy Simulation is employed with a precursor database model in Digital Wind Tunnel simulations. The average, fluctuation, minimum, and maximum façade loads are very well matched between the Experimental and Digital Wind Tunnels. Bennetsen, Thordal, & Capra, (2020) [6] Using CFD models, wind tunnel studies may be replicated and post-processed similarly. Both high-rises had mean surface pressures that were in line with the tests. The surface pressure coefficients at their lowest and highest points were in good agreement.

Karrar., Shyama, & Jassim (2020) [7] studied tall building wind load. Three-dimensional commercial programs were used for CFD modeling. ANSYS Fluent 19.0. Using finite volume to forecast tall building wind load using boundary conditions. The software investigated wind turbulence using LES and k-. The current numerical technique was confirmed by comparing drag and lift coefficients with wind tunnel experiments. Verma, Roy, Lather, & Sood's (2015) [8] study's structures are octagonal.

Mean area-weighted average wind pressures on building models are measured to explore the influence of 0°, 15°, and 30° wind incidence angles on wind pressure distribution. Fouad, Mahmoud, & Nasr, (2018) [9] The building's structural design incorporates the computation of wind loads. Codes for listed structures were derived from wind tunnel experiments but did not include all planned constructions. Experimental data is expensive and not always available; thus, designers must design wind parameters. Xing & Qian, (2018) [10] At Reynolds number 3900, one circular cylinder was simulated, and three circular cylinders were arranged in equilateral-triangular configurations. The numerical findings matched wind tunnel tests, proving the model's practicality. Two-dimensional models of three circular cylinders were used to simulate flow around the three high-rise structures in an equilateral-triangular arrangement.

Throughout history, humans have been fascinated by tall towers and buildings created for

protection and religious purposes. Modern tall building development started in the late 19th century for commercial and residential use. To be as near as possible to one another and the city center, companies are increasingly erecting tall commercial buildings, putting further strain on available land. High-rise commercial buildings in major cities are commonly seen as symbols of corporate power. Businesses and tourists have increased the demand for high-rise city center hotels. Rapid urbanization and a lack of available space have influenced cities' development. Due to rising land prices, the desire to keep urban sprawl to a minimum, and the need to keep workers productive, residential construction has increased. The research is about reducing the design by adopting CFD analysis compared to Wind Tunnel Testing.

3. Research Methodology

Combining mesh- and micro-scale models, this study used a geometric model. It's a micro-scale model in geometry, yet it spans a community site and a weather station many kilometers away. In contrast to a micro-scale model, this domain is much larger. Three structures made up the full-scale model. A full-scale model is larger than a microscale model. An overview of CFD use in modeling outdoor settings, "Best practice guideline for the CFD simulation of flows in the urban environment," and "Guidelines for practical applications of CFD to pedestrian wind environment around buildings" guided our study. ANSYS Fluent, a commercial CFD package, was utilized. CFX/ANSYS, PHOENICS, SIMSCALE, SIMFLOW, and STAR-CD can be used for research. This study employed FLUENT/ANSYS 19.0, a commonly used CFD code in industry and academics. The graphical interface is comparable to the commercial product mentioned above in design and functionality. Review ANSYS fundamentals before utilizing FLUENT/ANSYS. This chapter explains problem preparation, solution, and post-processing.

Flow chart of CFD geometry and meshes. After installing mesh-making software, the geometry is imported from CAD. The user generates the right mesh based on the geometry specifications. Ideally, a CFD solver should output the mesh. Mesh diagram: here.

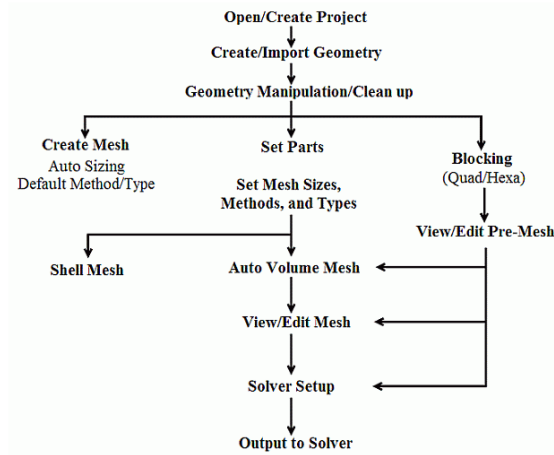


Figure 1: CFD Geometry and Meshing steps

3.1 Problem description

Tables demonstrate the dimensions of the building and the domain that need to be addressed for the problem of wind flow around an isolated building.

Table 1: Building Dimension

Width of Building	30 m
Depth of Building	30 m
Height of building	85 m

Table 2: Domain Dimension

Width of Domain	880 m
Depth of Domain	1730 m
Height of Domain	510 m

- A. Designing an ANSYS Workbench FLUENT Fluid Flow Analysis System
- B. Pre-Processing
 - a. Geometry
 - b. Meshing
 - c. Model set-up
- C. Processor
 - a. Solver
- D. Post Processing
 - a. Results

Begin by opening the ANSYS Workbench, creating a new fluid analysis, and then browsing through the list of files that ANSYS Workbench has produced. An overview of the ANSYS Workbench window may be seen in the figure below:

By opening the Windows Start menu, pick ANSYS 2019 Programs, then click ANSYS 2019 Workbench.

Start → All programs → ANSYS 2019 → Workbench

Create a new FLUENT fluid analysis system by double-clicking the Fluid Flow option in the Analysis System Toolbox.

Save the project.

File → Save

earlier, and different wind incidence angles. In this study, the k- ϵ (realizable) model has been used.

4.2. No. Of Models

For the present analytical study, there are 12 numbers of models that have been prepared, and the details of each model are listed below in the table:

Table 3: Number of Models prepared for the experiment

No.	Type	Quantity
	Square Isolated Building (Set up 1 to 3)	12

4. Illustrative Problem

Section I introduces wind and its effects on towering buildings. Section II covers CFD theory, application, and methodology. This chapter outlines the analytical models studied. In this work, CFD simulations were run using ANSYS 2019 R.2 (FLUENT) and compared to IS:875 (Part-3), 2015, for validation. This study will also evaluate the average pressure coefficient for buildings with setbacks, various cross-section shapes, and openings under isolated conditions. Changing the distance and wind incidence angle on buildings was studied. To conduct analytical studies, we assumed all structures were in terrain category 2.

4.1. Parameters Considered

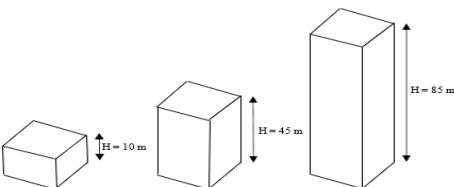
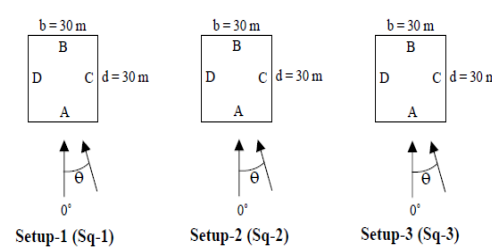
In the current study, eighteen different set-ups of building models have been considered. The set-up 1 to 4 was the isolated building with a basic square cross-section (plan shape) dimension 30m x 30m. Set-up 5 was an isolated building with a single and double setback. Setup 6 was building with varying cross-section shape along the height (33% height square + 66% height circular, 50% height square + 50% height circular and 66% height square + 33% height circular). Setup 7 was building with large opening (1%, 2%, 3%, 4% and 5% of surface area). Setup 8 was building with number of opening (1%, 2%, 3%, 4% and 5% of surface area). Set-up 9 was a three-building model with triangular orientation for different S/B ratios. Set-up 10 was three buildings model with row patterns for different S/B ratios. Setup 11 to 14 was two buildings model with different S/B ratios and different height of interference building (h : $H = 0.25, 0.5, 0.75, 1$). Where H is the height of the main structure and h is the height of the interference building. Set-up 15 was two buildings model with different S/B ratios and a large opening at interference building (1%, 2%, 3%, 4%, and 5% of surface area). Set-up 16 was two buildings model with different S/B ratios and several openings at interference buildings (1%, 2%, 3%, 4%, and 5% of surface area). S/B ratio for above mentioned building was 0.25, 0.5, 1, 1.5 and 2. The size of the object building and the interfering building was kept the same with dimensions of 30m x 30m x 85m except for two building models without opening. Wind incidence angle (β) has been varied from 0° to 90° with an increment of 15° in the anticlockwise direction. Wind forces on the building models are also measured for the building, as mentioned

4.3. Details Of Models

These are all of the building models that were utilized for the research. The Cross-sectional area (900 m²) and surface area (2550 m²) For comparative purposes, all 12 models are maintained the same. All models' dimension is in meter (m).

Table 4: Problem for validation Setup 1, 2 and 3

Model Shape	Face-A&C Width (m)	Face-B&D Depth (m)	H Height (m)	Side ratio	Aspect ratio
Square (Sq-1)	30	30	10	1	0.33
Square (Sq-2)	30	30	45	1	1.50
Square (Sq-3)	30	30	85	1	2.83



Setup-1 (Sq-1)

Setup-2 (Sq-2)

Setup-3 (Sq-3)

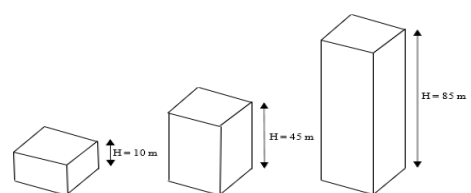


Figure 2: Building CFD Models

The present study is to carry out a CFD simulation on the building models which are already explained. Average values of wind pressure coefficients (C_p) and Drag forces are evaluated and presented in the present study.

The results are presented as pressure contour and velocity vector around the building.

5. Result & Discussion

A boundary layer wind tunnel research was conducted to determine the wind microclimate of potential development in Metro City. The pedestrian level wind environment at the site has been assessed and categorized according to the industry standard Lawson criteria for pedestrian comfort and safety thanks to the boundary layer wind tunnel investigation. Based on long-term data on wind frequency and pedestrian level wind speeds, the research identifies sites where wind speeds are likely to exceed acceptable levels for various popular pedestrian activities, as defined by the industry-standard Lawson criterion. Wind conditions are safe and pleasant for this kind of activity. The present study will carry out a CFD simulation on the building models already explained in the previous chapters. A total of three set-ups of building models have been considered for this study. Average values of wind pressure coefficients (C_p) and Drag forces are evaluated and presented in the present chapter. The results are presented as pressure contour and velocity vector around the building.

5.1. Set-up 1 (Square Isolated Building)

The dimension of set-up 1 (30m x 30m x 10m) is considered based on the height ratio and plan ratio of the building.

$$\text{Building height ratio} = \frac{h}{w} \leq \frac{1}{2}$$

$$\text{Building plan ratio} = 1 \leq \frac{l}{w} \leq \frac{3}{2}$$

In this set-up, an isolated building model was considered, and area average pressure coefficient (C_p) was calculated for all faces of the building at different wind incidence angles through a variation of 0° to 90° with an increment of 15° clockwise direction, and the results have been presented. Due to the direct influence of wind, the windward wall (Face-A) experiences positive pressure at an angle of zero degrees. The flow around the building's perimeter separates, resulting in negative pressure (suction) on the other three faces.

Table 5: Isolated building with varying wind incidence angle: average pressure coefficient for all four sides (Set-up 1)

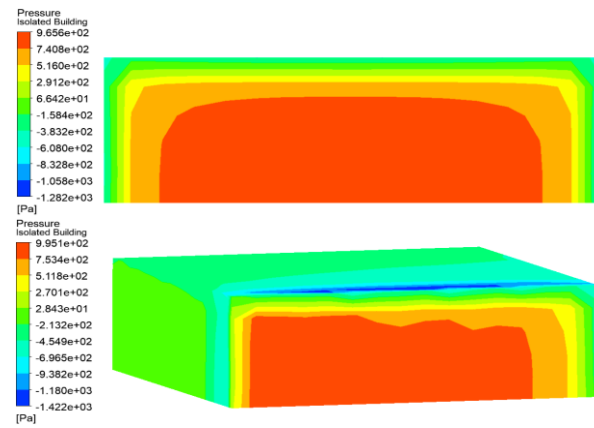
wind incidence angle (Deg)	Average Pressure Coefficient					
	Face A	Face B	Face C	Face D	max C_p	min C_p
0	0.625	-0.222	-0.383	-0.383	0.625	-0.383
15	0.661	-0.261	-0.514	-0.144	0.661	-0.514
30	0.566	-0.341	-0.531	0.139	0.566	-0.531
45	0.394	-0.438	-0.438	0.394	0.394	-0.438

60	0.139	-0.531	-0.341	0.566	0.566	-0.531
75	-0.144	-0.514	-0.261	0.661	0.661	-0.514
90	-0.383	-0.383	-0.222	0.625	0.625	-0.383

Table 6: Isolated building with varying wind incidence angle: average pressure coefficient for all four sides (Set-up 1)

FACE	Average Face Pressure Coefficient (C_p)		AS/NZ 1	ASCE
	CFD	IS-875 Part-3		
Face - A	0.625	0.7	0.9	0.7
Face - B	-0.222	-0.2	-0.6	-0.4
Face - C	-0.383	-0.5	-0.75	-0.6
Face - D	-0.383	-0.5	-0.75	-0.6

From center to edge, pressure on the windward wall decreases as it gets closer to the wind's edge at an incidence angle of zero degrees. IS-875 Part 3 2015 states that the windward face-A is subject to a mean area average pressure coefficient of 0.75. However, the table shows that it is 0.625. (Table). According to IS-875 (Part 3), the observed face average suction on the leeward side is negative 0.222 and negative 0.383, while the measured values are negative 0.02 and negative 0.50. CFD simulation results compared to those provided by IS-875 (Part 3) were fairly accurate for all of the building's faces. Figures. Depicts the highest area average pressure coefficient (C_p) for various faces at various wind incidences. The largest positive pressure coefficient (C_p) was found at an incidence angle of 15 degrees and 75 degrees, whereas the maximum negative pressure was found at an incidence angle of 30 degrees and 60 degrees. Pressure on the square model (Set-up 1) at wind incidence angles of zero, fifteen, thirty, and forty-five degrees is depicted in the figure.



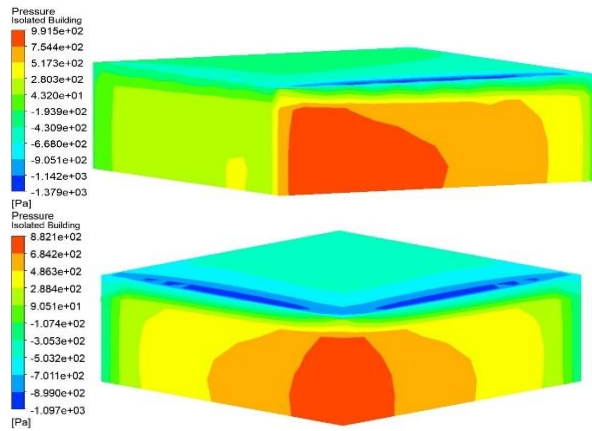


Figure 3: Contour of pressure for 0°, 15°, 30°, and 45° wind incidence angle (Set-up 1)

5.2. Set-up 2 (Square Isolated Building)

It is necessary to consider the building's height and plan ratio when calculating set-up 2's dimensions (30m x 30m x 45m).

$$\text{Building height ratio} = \frac{1}{2} \leq \frac{h}{w} \leq \frac{3}{2}$$

$$\text{Building plan ratio} = 1 \leq \frac{l}{w} \leq \frac{3}{2}$$

An isolated building model was used in this setting, and the area average pressure coefficient (C_p) was determined for all sides of the structure at varied wind incidence angles spanning a range of 0 to 90 degrees with an increment of 15 degrees clockwise.

Table 7: Variation in wind incidence angle affects the average pressure coefficient on all four sides of an isolated building (Set-up 2)

Wind incident angle (Degree)	Average Pressure Coefficient (C_p)					
	Face A	Face B	Face C	Face D	Max +ve	Min -ve
0°	0.65	-0.33	-0.46	-0.46	0.65	-0.46
15°	0.69	-0.37	-0.43	-0.34	0.69	-0.43
30°	0.60	-0.45	-0.48	0.09	0.60	-0.48
45°	0.42	-0.47	-0.47	0.42	0.42	-0.47
60°	0.09	-0.48	-0.45	0.60	0.60	-0.48
75°	-0.34	-0.43	-0.37	0.69	0.69	-0.43
90°	-0.46	-0.46	-0.33	0.65	0.65	-0.46

Table 8: At 0 wind incidence angle, CFD simulation results were compared to those from the wind standard of India.

FACE	Average Face Pressure Coefficient (C_p)		
	CFD	IS-875	AS/NZ
			ASCE

		Part-3	1170.2	0.2
Face - A	0.652	0.7	0.7	0.7
Face - B	-0.33	-0.25	-0.6	-0.6
Face - C	-0.46	-0.6	-0.55	-0.8
Face - D	-0.46	-0.6	-0.55	-0.8

Compared to the IS-875 (Part 3) provision of 0.7, the windward face-A is subject to positive pressure when the wind incidence angle is 0 (Table) (Table). For the front face of the structure, it is evident that the average pressure on the surface falls as the wind incidence angle increases. At a wind incidence angle of 90 degrees, it turns negative and becomes suction. Leeward and side faces have average suction values of -0.331 and -0.463, whereas the IS-875 (Part 3) values are -0.25 and -0.6, respectively. The maximum area average pressure coefficient (C_p) for different sides was plotted with varied wind incidence, as shown in Fig. The greatest positive pressure coefficient (C_p) was found at 15 and 75 wind incidence angles, whereas the maximum negative pressure was found at 30 and 60. As seen in the figure, there is a pressure contour on the square model (Set-up 2) for wind incidence angles of zero, fifteen, thirty, and forty-five degrees.

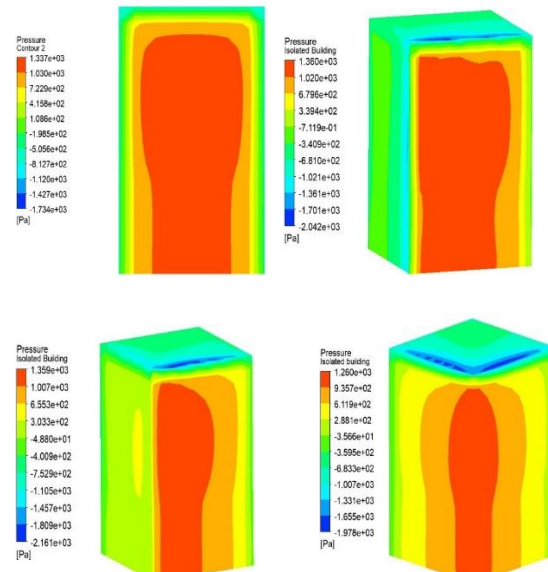


Figure 4: Contour of pressure for 0°, 15°, 30°, and 45° wind incidence angle (Set-up 2)

5.3. Set-up 3 (Square Isolated Building)

Set-up 3's dimensions (30 x 30 m x 85 m) are determined by the building's height to plan ratio.

$$\text{Building height ratio} = \frac{3}{2} < \frac{h}{w} < 6$$

$$\text{Building plan ratio} = 1 \leq \frac{l}{w} \leq \frac{3}{2}$$

These findings are displayed in Table and Fig. for an

isolated building model at various wind incidence angles ranging from 0° to 90° with a 15° clockwise increment. The results of this analysis are summarized in the following tables and figures.

Table 9: All four sides of an isolated structure with varying wind incidence angles have the same average pressure coefficient (Set-up 3)

Wind incidence angle (Degree)	Average Pressure Coefficient (Cp)					
	Face A	Face B	Face C	Face D	Max +ve	Min -ve
0°	0.750	-0.31	-0.54	-0.54	0.750	-0.54
15°	0.708	-0.41	-0.48	-0.41	0.708	-0.48
30°	0.648	-0.49	-0.54	0.129	0.648	-0.54
45°	0.492	-0.53	-0.53	0.492	0.492	-0.53
60°	0.129	-0.54	-0.49	0.648	0.648	-0.54
75°	-0.41	-0.48	-0.41	0.708	0.708	-0.48
90°	-0.54	-0.54	-0.31	0.750	0.750	-0.54

Table 10: Set-up 3 at 0 angles of incidence compares CFD simulation results with national wind standards to determine which building's four sides are most affected by the wind.

FACE	Average Face Pressure Coefficient (Cp)			
	CFD	IS-875 Pa 3	AS/NZ 1170.2	ASCE 0.2
Face - A	0.75	0.8	0.8	0.8
Face - B	-0.316	-0.25	-0.5	-0.5
Face - C	-0.546	-0.8	-0.65	-0.7
Face - D	-0.546	-0.8	-0.65	-0.7

Against the IS-875 (Part 3) requirement of 0.8, the windward face-A is under positive pressure when the wind incidence angle is 0° (Table) (Table). For the building's front face, it is evident that the average surface pressure falls as the wind incidence angle increases. At a wind incidence angle of 90° degrees, it turns negative and becomes suction. If you look at the IS-875 (Part 3), you can see that the leeward face suction average is 0.316 and the side face suction average is 0.546. The maximum area average pressure coefficient (Cp) for different sides was plotted with varied wind incidence as shown in Fig. Cp was highest at 0° and 90° degrees of wind incidence angle, whereas Cp was highest at 0° degrees of the wind incidence angle in this case.

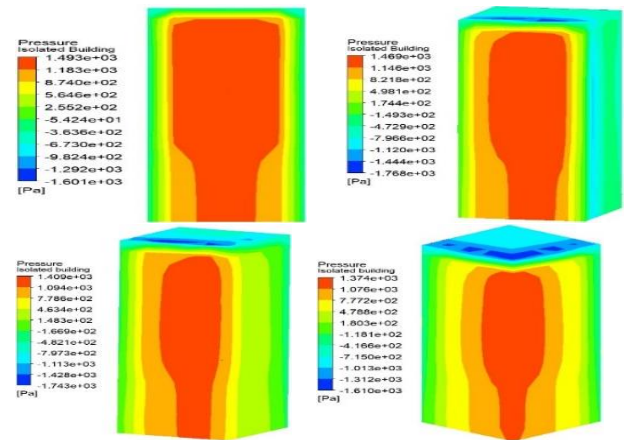


Figure 5: Contour of pressure for 0° , 15° , 30° , and 45° wind incidence angle (Set-up 3)

There is a depiction in Figure 2 showing the contour of pressure on the square model's faces (Set-up 2) for wind incidence angles of 0° , 15° , 30° , and 45° degrees. This research aims to do CFD simulations on the building models described in Chapter 4 of the book. Three different configurations of building models were taken into account for this investigation. The current chapter evaluates and presents average wind pressure coefficients (Cp) values and drag force. Results are shown as a pressure contour around the building and a velocity vector. To determine the overall drag force of setback buildings for wind incidences ranging from 0° to 90° , estimate the average pressure coefficient on the various surfaces of single and double setback buildings, and compare it to an isolated square structure (Set-up 3). Tables and figures indicate the comparability of the findings.

A. Tower A (or) B

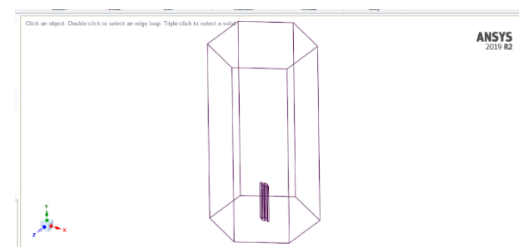


Figure 6: Tower One Geometry

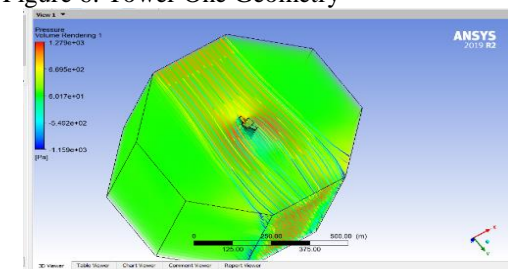


Figure 7: pressure-volume rendering

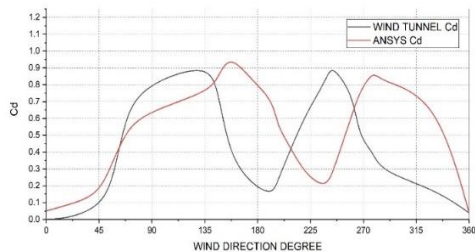


Figure 8: Tower A Wind Tunnel vs. Ansys CD

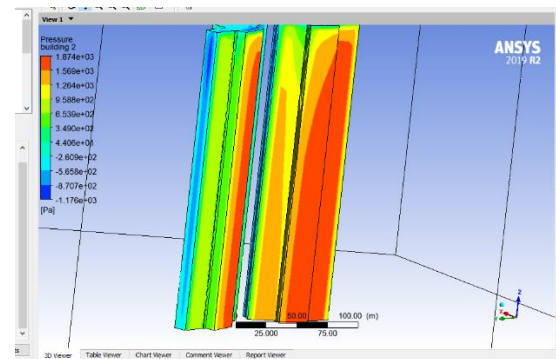


Figure 12: Two Towers Pressure Couture

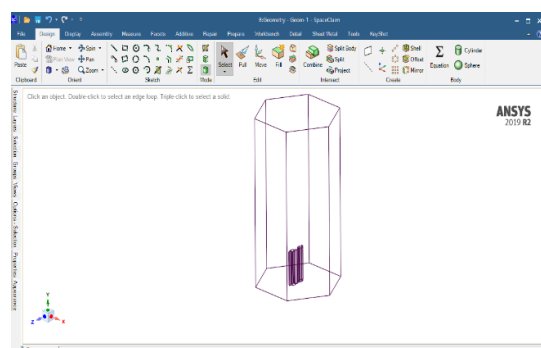


Figure 9: Two Towers Geometry

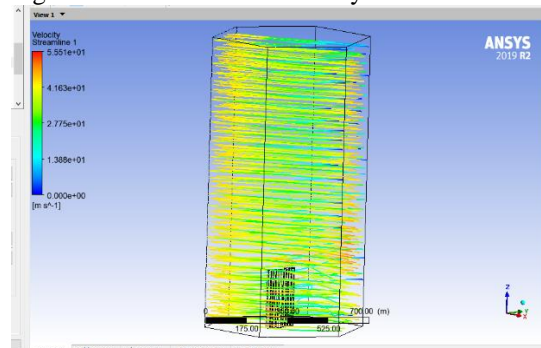


Figure 10: Velocity streamline of two towers

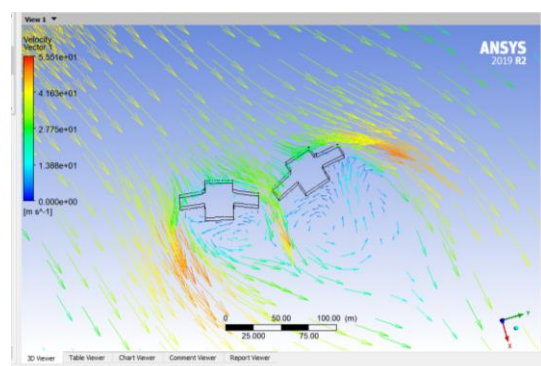


Figure 11: Velocity vector and wind pressure of two towers (A)

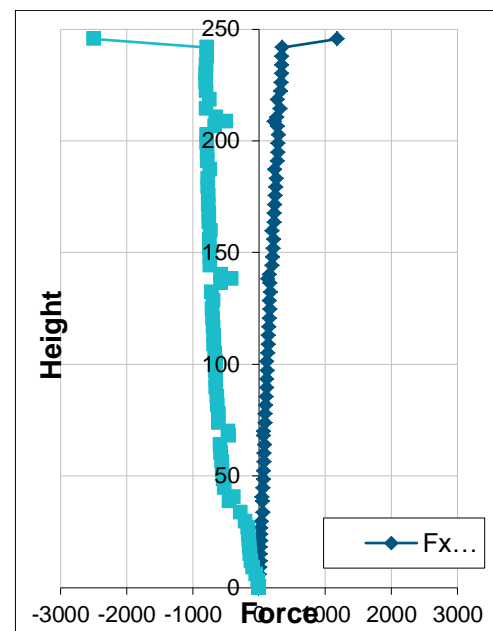
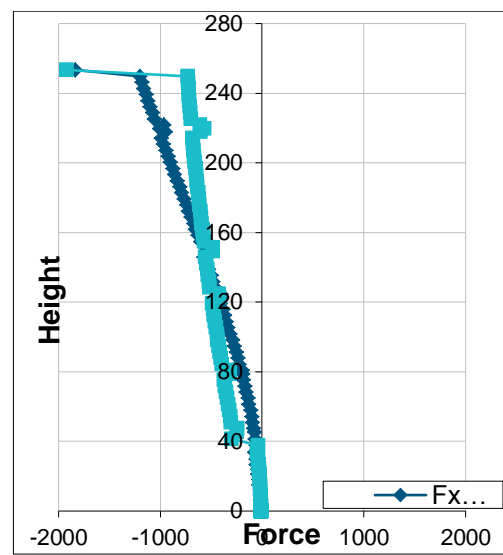
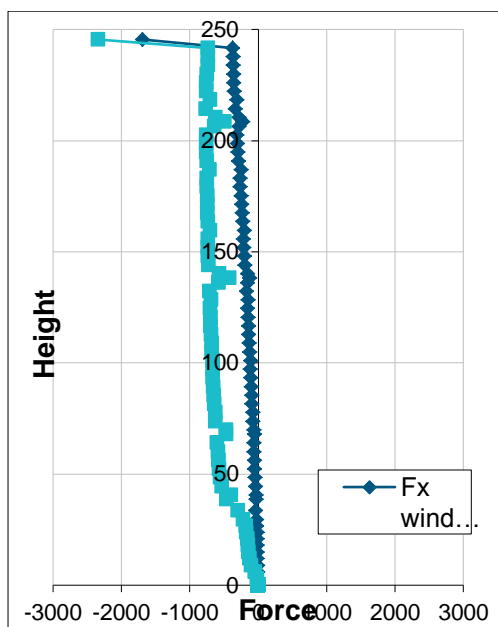


Figure 13: Tower A Force Analysis



C. Tower C

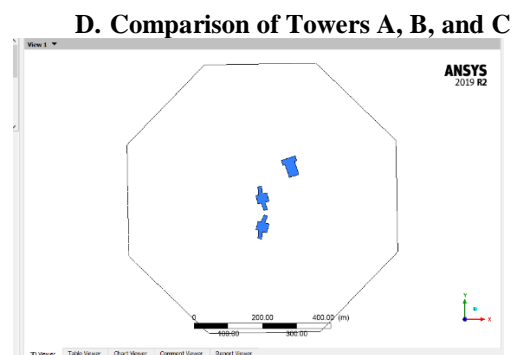
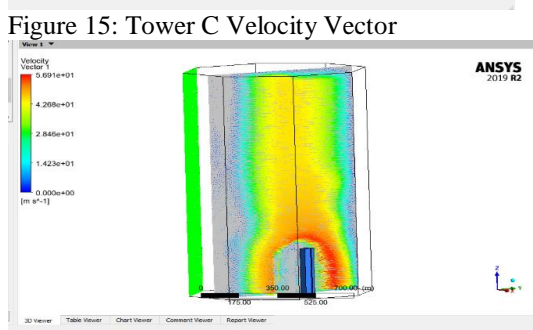
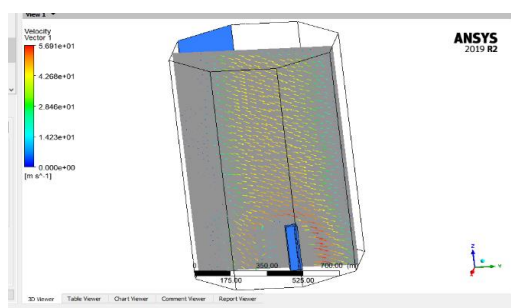
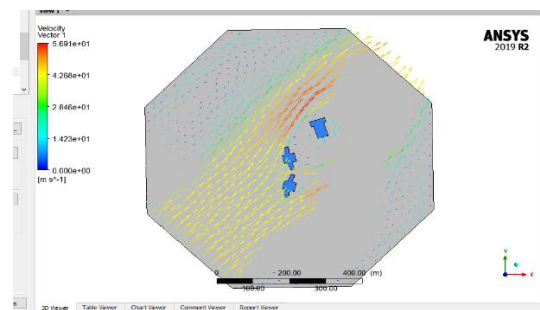
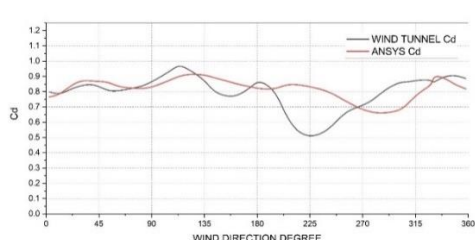


Figure 19: Top View Three Towers



E. Comparison of Tower A & C



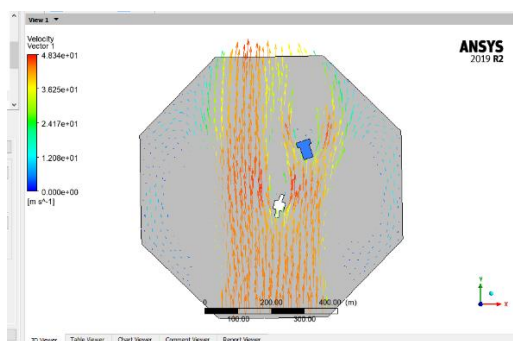


Figure 21: Tower A & C Velocity Vector

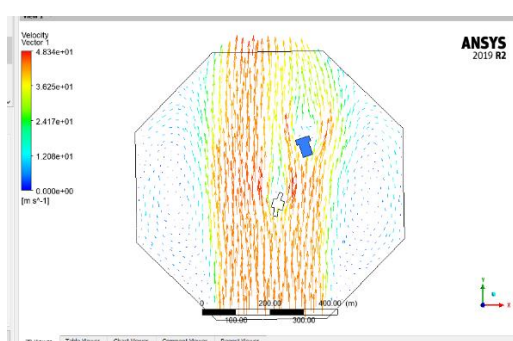


Figure 22: Velocity Vector top view of Tower A & C

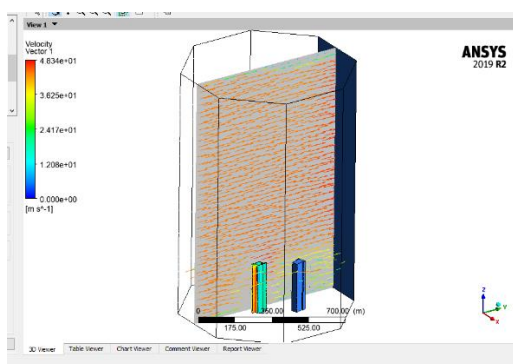


Figure 23: 3D of the inlet, outlet, and velocity vector of Tower A and C

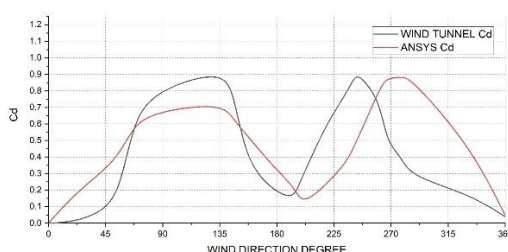


Figure 24: Drag coefficient comparison of Ansys and Wind tunnel analysis

Globally recognized wind rules focus on wind loading, not ambient wind flows in the built environment. Standard engineering approaches or handbooks can't adequately examine the complex environmental wind fluxes that affect pedestrians. Numerical/computational approaches

like computational fluid dynamics don't work well for built-environment wind flows. Consequently, boundary layer wind tunnel research was used to properly measure the pedestrian wind environment, notably in the following critical areas:

- Footpaths to the building
- Entranceways

For a wide range of pedestrian activities, wind speed-up factors at and around the site and long-term wind frequency records are combined to assess the possibility of local wind speeds exceeding comfort and safety norms at the site. Threshold wind speeds depend on several factors. A model-scale boundary layer wind tunnel can test a wide range of wind directions for increased speed. The wind statistics recorded by a meteorological station are transferred to where it is most likely to blow.

Also included are photos demonstrating the model's size, construction, and operation in a wind tunnel. When utilized at full size, the model's 1:400 scale accurately depicts the complexities that can influence local and global wind flows. It is also possible to reproduce the wind's turbulence on a huge scale.

6. Conclusion

ANSYS' commercial CFD software was utilized when showing flow patterns and pressure distribution around the tall buildings. Numerical analysis of the wind flow was carried out using pre-defined models. The computational result and the experimental data for the wind incidence angle are in good agreement.

Variations have been observed in wind tunnel testing and CFD Ansys tests, but to reduce design and testing costs, CFD is recommended strongly for the initial approximation results.

The major difference between wind tunnel testing and CFD testing is the limitations with surface roughness; it is considered while testing in the wind tunnel, but the same gets complex to multiple levels while testing in CFD.

Real-world terrains can be designed and tested seamlessly in wind tunnels. Complicated in CFD designing and testing is massively time-consuming.

Regarding cost and pricing, wind tunnel testing is very expensive. The same gets reduced with CFD by 70%.

6.1. Future Scope

The research can further be taken forward by including Surface roughness while designing and testing in CFD to achieve an optimized outcome. Using other 2D and 3D in combination can result in optimized testing and reduces the cost by several times. These tools help include real-world terrains to achieve a clearer picture of the wind interfaces.

References

- [1] . S. Thordal, J. C. Bennetsen and H. H. Koss, "Review for practical application of CFD for the determination of wind load on high-rise buildings," Journal of Wind Engineering and Industrial Aerodynamics, pp. 155-168, 2019.
- [2] V. R. Shinde and V. S. Shingade, "Review on Computational Evaluation of Wind Pressure on Tall Buildings using CFD and S_d ," INTERNATIONAL JOURNAL OF ENGINEERING RESEARCH & TECHNOLOGY (IJERT), pp. 1-6, 2018.
- [3] K. Hu, S. Cheng and Y. Qian, "CFD Simulation Analysis of Building Density on Residential Wind Environment," Journal of Engineering Science & Technology Review, pp. 1-8, 201
- [4] X. F. Yu, Z. N. Xie, J. B. Zhu and M. Gu, "Interference effects on wind pressure distribution between two high-rise buildings," Journal of Wind Engineering and Industrial Aerodynamics,, pp. 188-197, 2015.
- [5] P. K. Sharma and S. R. Parekar, "Drag Coefficient of Tall Building by CFD Method using ANSYS," IRJET Journal, pp. 1-6, 2019
- [6] J C. Bennetsen, M. S. Thordal and S. Capra, "Towards a standard CFD set-up for wind load assessment of high-rise buildings: Part 2–Blind test of chamfered and rounded corner high-rise buildings," Journal of Wind Engineering and Industrial Aerodynamics, p. 104282, 2020
- [7] W. S. Karrar., A. M. Shyama and M. Jassim, "High-rise building wind analysis using computational fluid dynamics and dynamic analysis using etabs program," International Journal, pp. 1-8, 2020
- [8] S. K. Verma, A. K. Roy, S. Lather and M. Sood, "CFD simulation for wind load on octagonal tall buildings," Int J Eng Trends Technol, pp. 211-216, 2015
- [9] N. S. Fouad, G. H. Mahmoud and N. E. Nasr, "Comparative study of international codes wind loads and CFD results for low rise buildings," Alexandria engineering journal, pp. 3623-3639, 2018.
- [10] . Xing and J. Qian, "CFD analysis of wind interference effects of three high-rise buildings," Journal of Asian Architecture and Building Engineering, pp. 487-494, 2018.